JOURNAL OF GUIDANCE, CONTROL, AND DYNAMICS
Vol. 27, No. 2, March–April 2004

Miss Distance Error Analysis of Exoatmospheric Interceptors

Hari B. Hablani* and David W. Pearson†
The Boeing Company, Huntington Beach, California 92647-2099

A miss distance error analysis of exoatmospheric interceptors with liquid divert thrusters in endgame is presented. The analysis relates miss distance uncertainty to 1) infrared/electrooptic seeker noise, 2) seeker latencies caused by image processing and motion compensation and integration to detect the target on the focal plane, 3) seeker scan angle measurement errors of gyro, 4) range error or time-to-go error, and 5) filtration of all these errors through a Kalman filter for estimating the line-of-sight (LOS) rates. With the relationships developed, the missile designer/analyst can predict a probable miss distance with the hardware parameters of the selected divert thrusters and sensor suite, as well as software parameters of the selected guidance policy. The analyst can also arrive at the LOS rate estimation accuracy requirements about the azimuth and elevation axes, to be achieved by a tracking Kalman filter for specified miss distance statistics. The analysis provides insight and predicts reliably the miss distances expected from Monte Carlo simulations and hardware-in-the-loop laboratory tests.

I. Introduction

MISS distance error analysis of air missiles seems to be well understood,[1,2] but that of exoatmospheric interceptors equipped with infrared sensors and liquid divert thrusters appears to be lagging behind. To be sure, Refs. 3–6 provide a system engineer design tools to arrive at hardware/software requirements for exoatmospheric interceptors to meet a specific miss or hit accuracy without the use of an elaborate trajectory simulation. However, these references do not specifically address unique features of exoatmospheric interceptors with liquid propulsion systems. This paper attempts to fill this gap.

A brief review of the pertinent contributions of the past follows. Murtaugh and Criel[7] considered proportional navigation with a deadzone, and they related throttleable acceleration of the engine with propellant weight and miss distance. Though insightful and fundamental, divert thrusters of constant acceleration, seeker noise, estimation errors, and inherent delays in the system are not considered. Salmon and Heine[3] performed a tradeoff between missile controllability and sensor noise by using reachable sets analysis. However, they assumed accurate relative range measurements of the target and, thus, ignored an important parameter, the time-to-go error. More recently, Zarchan[4] developed normalized miss distance curves for exoatmospheric interceptors and modeling delays in guidance and control system as a fifth-order binomial and accounted for acceleration saturation. However, Ref. 4 is limited to proportional navigation and is not applicable to divert thrusters of constant acceleration, with a threshold for commanded acceleration. Spencer and Moore[5] applied the covariance propagation technique for statistical analysis of miss distance sensitivity of exoatmospheric interceptors. However, Ref. 5, too, is not concerned with the pulsed proportional navigation guidance. Lawrence[6] conducted a miss distance error analysis of exoatmospheric interceptor guidance. Though an excellent study pertinent to this paper, like Ref. 3, it does not cover miss distance uncertainty arising from the time-to-go error, nor is it concerned with the relationships between divert thrust, pulse width, line of sight (LOS) rate decrement by minimum impulse bit, and a threshold for the commanded acceleration. The present study considers all of the aspects of miss distance error analysis not covered in Refs. 3–6.

The remainder of this paper comprises five sections. In Sec. II, reasonable bounds are developed of LOS rate estimation accuracy requirement for the parameters of the strategic interceptor at hand. In Sec. III, analysis and estimates of uncertainty in miss distance caused by LOS rate estimation error $\delta\omega$, time-to-go estimation error δt_{go}, and closing velocity estimation error δV_{cl} are presented. The growth, if any, in the miss distance estimation error as the interceptor approaches the target is formulated and examined. Because the LOS rate estimation error contributes significantly to the miss distance uncertainty and because this error arises from the gyro and electrooptic sensor measurements of azimuth and elevation angles of the target relative to an inertial frame, the sources of this error are identified, formularized, and elucidated in Sec. IV. Dependence of the miss distance uncertainty on the estimation errors $\delta\omega$, δt_{go}, and δV_{cl} is illustrated and compared with Monte Carlo simulation results in Sec. V. Section VI concludes the paper.

II. LOS Rate Estimation Accuracy Requirement

In Ref. 8, it is shown that an incremental velocity $\Delta V = a_{\text{div}}\tau_w$ in a τ_w duration $t_k \le t \le t_{k+1}$ will decrease the LOS rate by $\Delta\omega$ given by

$$\Delta\omega \approx \frac{a_{\text{div}}\tau_w}{V_{\text{cl}}t_{\text{go},k+1}} \tag{1}$$

where a_{div} is the divert acceleration, V_{cl} is the closing velocity, $t_{\text{go},k+1}$ is the time-to-go at time $t = t_{k+1}$, and k denotes the kth sample.

Equation (1) reveals the required accuracy of the LOS rate estimate to be provided by a Kalman filter to achieve a specified miss distance. With each pulse of a 15 or 25 ms width near the closest approach, the LOS rate decreases abruptly, and to minimize the miss distance effectively, the LOS rate estimates must be able to track the true LOS rate with small errors in the presence of seeker latencies and noise and gyro and accelerometer measurement errors. Lawrence[6] developed an LOS rate accuracy requirement of $\delta\omega \le a_{\text{div}}/(2V_{\text{cl}})$ which, for $a_{\text{div}} = 30\,\text{m/s}^2$ and $V_{\text{cl}} = 7300\,\text{m/s}$, yields $\delta\omega \le 2$ mrad/s. To check the adequacy of this requirement, consider the following: For a miss distance requirement of 10 cm at $t_{\text{go}} = 0.1s$ (and, therefore, $r = V_{\text{cl}}t_{\text{go}} = 730$ m), the relationship zero effort miss (ZEM) $= \omega r t_{\text{go}}$ imposes an LOS rate as small as $\omega = 1.37$ mrad/s. Furthermore, if this is to be the residual rate after a 15-ms pulse from the previous sample, $t_{\text{go}} = 0.125$ to 0.1 s, the LOS rate decrement $\Delta\omega$ then will be 0.5 mrad/s. In view of 1.37 mrad/s LOS rate and 0.5 mrad/s LOS rate decrement, the LOS rate estimation accuracy requirement of $\delta\omega \le 2$ mrad/s is clearly inadequate. Instead, a requirement of, for example, 0.1 μrad/s (100 μrad/s) appears more

Received 13 February 2001; presented as Paper 2001-4279 at the AIAA GNC Conference, Montreal, Canada, August 2001; revision received 24 September 2003; accepted for publication 26 September 2003.

*Technical Fellow, Flight Systems Design and Analysis. Associate Fellow AIAA.

†Chief System Engineer, Ground Based Interceptor/Exoatmospheric Kill Vehicle Program.

suitable. The requirement developed in Ref. 6 is lax because it ignores discrete divert pulses, t_{go} error or range error, seeker latency, and any other latencies. Also, in Ref. 6 it is assumed that the divert remains on for the remaining t_{go} and produces a time-varying acceleration as required by the proportional navigation guidance policy, instead of constant acceleration produced by a pulse.

III. Miss Distance Estimation Error Analysis

In a planar endgame, miss distance is given by $\text{ZEM} = \omega r t_{go}$. Hence, accuracy of the miss distance estimate is a function of the accuracy of the estimates of ω, r, and t_{go}. In this section, we will examine how the estimation errors $\delta\omega$, δt_{go}, and δV_{cl} influence a ZEM estimate. Lawrence,[6] in contrast, considers only $\delta\omega$ in his miss distance error analysis. The LOS rate ω is estimated by a Kalman filter by processing noisy LOS angle measurements from the seeker focal plane with attitude measurements from a strapdown gyro. See Ref. 9 for a similar procedure for air missiles. The estimate of ω, denoted $\hat{\omega}$, has an estimation error $\delta\omega$ such that $\hat{\omega} = \omega + \delta\omega$. The estimation accuracy of ω depends on, among other things, the accuracy of our knowledge of t_{go}, which may not be high. Moreover, t_{go} may not be estimated by the Kalman filter. Hence, the accuracy of the time-to-go estimate is a function of in-flight target updates. Though the proportional navigation guidance scheme has the appearance of not requiring t_{go} for guidance, ω must still be estimated. Because this estimation is to be performed by a Kalman filter and not by differencing two successive LOS angle measurements, the Kalman filter requires the current range estimate, or equivalently, the estimated time-to-go $\hat{t}_{go}$, to transform the Cartesian state vector to a polar state vector and vice versa and to calculate the t_{go}-dependent transition matrix.[8,10] Thus, the t_{go} estimation error δt_{go} influences $\hat{\omega}$ and $\delta\omega$.

Ineffective Time-to-Go

We now introduce an important parameter, $t_{go,ineff}$, that affects the miss distance. It is the remaining time-to-go during which the LOS rate estimation errors, the lags (or latencies) in processing seeker electrooptic signals, the delay in transporting the LOS rate estimates from the Kalman filter to the guidance module, the time-to-go error, thruster delays, etc., are all so overwhelming that they render the guidance system ineffective in decreasing the miss distance any further, and therefore, the guidance is better turned off. The parameter $t_{go,ineff}$ pertains to the quantity $r_{critical}$ introduced in Ref. 6, except that $r_{critical}$ therein is a function of the LOS rate uncertainty only and ignores the other error sources just enumerated. The concept of $t_{go,ineff}$ is not new. While conducting finite time stability of proportional navigation (singular at $t_{go} = 0$) using the circle criterion, Gurfil et al.[11] introduced a parameter called the shortest time-to-go τ^* for which the guidance divergence might occur for a given flight time and system parameters. Indeed, τ^* is the same as $t_{go,ineff}$. Similarly, Shneydor[12] analyzes stability of the guidance system in the presence of delays by employing frozen range, Nyquist criterion, and Popov criterion and relates $t_{go,ineff}$ with the time delay.

Use of Refs. 4, 11, and 12 helps quantify the parameter $t_{go,ineff}$. In Ref. 4, the lags in the guidance system are modeled as a time constant T_L comprising five $T_L/5$ delays: $T_L/5$ for the seeker, $T_L/5$ for filtering noise in the measured LOS rate, and $3T_L/5$ for the gyros, thrusters, and any other flight control delays. In Ref. 11, the guidance and control system is modeled as a product of n first-order systems in one example and a product of a first-order and a second-order system in a different example. However, guidance, navigation, and control operation of a real exoatmospheric interceptor with a liquid propulsion system is far more complicated than the first- and second-order transfer functions. The seeker and gyro operation of a strategic interceptor to measure LOS angle is elaborated in Sec. IV, and Table 1 presents a summary of relationships between the lag T_L and $t_{go,ineff}$ based on the stability analyses in Refs. 4, 11, and 12. As illustrated in Ref. 11, the frozen-range and Nyquist stability analyses yield a shorter $t_{go,ineff}$ than the Popov and circle criteria do. Nyquist criterion shows that, as the number n of the first-order lags in the complete closed-loop path increases from 2 to ∞ (sluggish closed loop), keeping the total delay T_L the same, the $t_{go,ineff}$ increases to the limit $0.64NT_L$, where N is navigation ratio. The ineffective range, $r_{go,ineff} = t_{go,ineff} V_{cl}$, increases correspondingly. For $N = 4$, the $t_{go,ineff}$ ranges from T_L to $2.55T_L$. Popov stability analysis and circle criterion predict a conservative limit, $t_{go,ineff} = 4T_L$. The concept of $t_{go,ineff}$ is applied in the rest of the paper to predict miss distance for given guidance and control parameters.

Table 1 According to stability analyses[11,12] $t_{go,ineff}$ and r_{ineff}

			$N = 4$	
Method	$t_{go,ineff}$	r_{ineff}	$t_{go,ineff}$	r_{ineff}
Frozen range and a double-lag system with each lag $= T_L/2$	$0.25NT_L$[a]	$0.25NV_{cl}T_L$	T_L	$V_{cl}T_L$
Nyquist criterion				
Double-lag ($n = 2$)	$0.25NT_L$	$0.25NV_{cl}T_L$	T_L	$V_{cl}T_L$
Fourth-order lag ($n = 5$), each lag equal to $T_L/4$	$0.48NT_L$	$0.48NV_{cl}T_L$	$1.92T_L$	$1.92V_{cl}T_L$
Sluggish guidance and flight control loop ($n = \infty$)	$0.64NT_L$	$0.64NV_{cl}T_L$	$2.55T_L$	$2.55V_{cl}T_L$
Popov and circle criteria	NT_L	$NV_{cl}T_L$	$4T_L$	$4V_{cl}T_L$

[a] T_L = total lag in the system.

Miss Distance Uncertainty

The miss distance uncertainty δZEM is derived by taking variation of $\text{ZEM} = \omega t_{go}^2 V_{cl}$,

$$\delta\text{ZEM} = \delta\omega V_{cl} t_{go}^2 + 2\omega V_{cl} t_{go} \delta t_{go} + \omega t_{go}^2 \delta V_{cl} \tag{2}$$

Our objective is to determine δZEM when $t_{go} = t_{go,ineff}$ and its evolution afterward. Suppose ω_0 is the true or nominal LOS rate at $t_{go} = t_{go,ineff}$ and $\delta\omega_0$ is its estimation error. To determine $\delta\omega(t)$, recall that, on a near-collision course, the LOS rate ω is governed by the classical equation of motion[7]

$$\dot{\omega} \approx (2/t_{go})\omega - a_{div}/r \tag{3}$$

where miss distance is along the Y_{LI} axis, the relative range r is along the x_{LI} axis, and a_{div} is the divert acceleration along the y_{LI} axis.

We now take the variation of Eq. (3), with $a_{div} = 0$, and arrive at

$$\delta\dot{\omega} = (2/t_{go})\delta\omega - 2\omega\left(\delta t_{go}/t_{go}^2\right) \tag{4}$$

for which the initial conditions are as follows: At $t = 0$, $t_{go} = t_{go,ineff}$, $\omega = \omega_0$, $\delta\omega = \delta\omega_0$, and $\text{ZEM} = \omega_0 V_{cl} t_{go,ineff}^2$. Equation (4) is more general than its counterpart Eq. (15) in Ref. 6, in that Eq. (4) includes the δt_{go} error. Because $\omega t_{go}^2 = \omega_0 t_{go,ineff}^2$, substitute the LOS rate $\omega(t)$ from this integral in Eq. (4), and integrate the equation with the initial conditions stated earlier. We then arrive at

$$\delta\omega(t) = \left(t_{go,ineff}^2/t_{go}^2\right)\delta\omega_0 - 2\left(\omega_0 t_{go,ineff} t/t_{go}^3\right)\delta t_{go} \tag{5}$$

where the instantaneous time-to-go is $t_{go} = t_{go,ineff} - t$ and the closest approach takes place when $t_{go} = 0$ and $t = t_{go,ineff}$. We now substitute the solution $\delta\omega(t)$, Eq. (5), in Eq. (2) and arrive at

$$\delta\text{ZEM}(t) = \delta\omega_0 V_{cl} t_{go,ineff}^2 + 2\omega_0 V_{cl} t_{go,ineff} \delta t_{go} + \omega_0 t_{go,ineff}^2 \delta V_{cl} \tag{6}$$

which, perhaps not surprisingly, is constant, equal to its initial value at $t = 0$, just as the ZEM is constant, equal to its initial value $\text{ZEM}_{ineff} = \omega_0 V_{cl} t_{go,ineff}^2$ at $t_{go} = t_{go,ineff}$ and $t = 0$. The first term in the right side of Eq. (6) is the same as the ZEM uncertainty, Eq. (22) of Lawrence,[6] caused by the LOS rate uncertainty; the remaining two terms arise from the time-to-go estimation error and the closing velocity estimation error.

Because estimating the inertial LOS rate from the seeker focal plane measurement and gyro measurement of inertial attitude of the focal plane is the principal purpose of the Kalman filter in a guidance system, and because the LOS rate estimation error affects

the miss distance profoundly, we next focus on 1) the LOS angle measurement process of exoatmospheric interceptors scanning the celestial sphere, 2) the errors in this measurement process, and 3) LOS rate estimation errors of the Kalman filter.

IV. LOS Rate Estimation Error

It will be shown in this section that the LOS rate estimation process is far more complicated than the frequently used assumption in a large number of papers that the measured and the true LOS rates are related by a simple first-order transfer function.

LOS Angle Measurement Using a Scanning Seeker and a Gyro

We will first describe the process of measuring azimuth and elevation angles of the target relative to an inertial frame and the associated noise characteristics. These inertial measurements, the azimuth $\theta_{z,m}$ and the elevation $\theta_{y,m,}$ relative to a local inertial frame, are obtained by combining the measurements from a seeker, which determines the coordinates of the target image on the focal plane with respect to the focal plane center, and from a strapdown gyro, which measures the focal plane orientation in the inertial frame.[5,9] Figure 1 shows this process for the azimuth angle θ_z about the z_{LI} axis. The angle θ_z consists of θ_{zb} and θ_{zs}, where θ_{zb} is the attitude of the interceptor body measured by the gyro relative to an inertial frame and θ_{zs} is the angle locating a target image on the focal plane measured from the focal plane center along the y_{LI} axis (actually, along the interceptor body axis y_b very nearly parallel to y_{LI}). Likewise, the elevation angle θ_y about the y_{LI} axis consists of θ_{yb}, the pitch attitude, and θ_{ys}, equivalent to the location of the target image along the $-z_{LI}$ axis (actually along a very nearly parallel $-z_b$ axis of the interceptor body) measured from the focal plane center. Thus, elevation

$$\theta_y = \theta_{yb} + \theta_{ys} \tag{7}$$

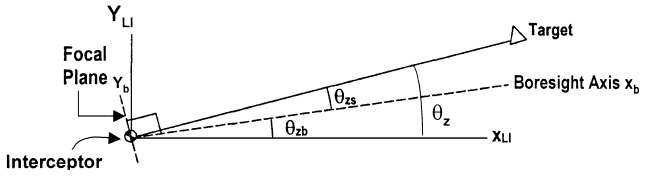

Fig. 1 LOS azimuth angle measurement with a seeker and a gyro (local inertial frame, planar analysis).

and azimuth

$$\theta_z = \theta_{zb} + \theta_{zs} \tag{8}$$

The focal plane angles θ_{ys} and θ_{zs} are determined by a very complex electrooptics process whose salient features are shown in Fig. 2. If the endgame guidance sampling rate is f hertz (40 Hz, in this study), the gyro may output the incremental attitude change of the interceptor at $10f$ (400-Hz) frequency but with some error and delay. For example, a gyro may produce the following incremental attitude change, $\Delta\theta_{400}$, over a time period of 2.5 ms obtained by a weighted average of nine 2000-Hz measurements of the interceptor incremental angles about the axis in consideration:

$$\Delta\theta_{400} = \Delta t_{2000}(\omega_{k-1} + 2\omega_{k-2} + 3\omega_{k-3} + 4\omega_{k-4} + 5\omega_{k-5} + 4\omega_{k-6} + 3\omega_{k-7} + 2\omega_{k-8} + \omega_{k-9})/5 \tag{9}$$

where $\Delta t_{2000} = 0.5$ ms. The nine 2000-Hz samples span a 4.5-ms interval or nearly two 400-Hz sample intervals, and therefore, the $\Delta\theta_{400}$ gyro measurement has a delay of $\sim$2.5 ms. Though the incremental angle is quantized, the quantization errors will not be discussed here. Next, as described, in Ref. 13, the seeker may perform a scan motion to collect and integrate photons emitted by the target at, for example, $100f$ frequency. To compensate for the scan motion, the seeker receives attitude measurements from the gyro at $10f$ frequency, one measurement per packet of 10 focal plane images, and determines, after extensive electrooptic computations, the centroid of the target image on the focal plane at the guidance frequency of f hertz. The data flow in Fig. 2 delineates this process of measuring the focal plane coordinates of the target image aided by the gyro with a technique called motion compensation and integration. At the end of each f hertz sample interval ($1/f$ second, 25 ms in this work), the seeker arrives at the measurements θ_{ys} and θ_{zs}, which locates the target relative to the focal plane axes at the start of that sample, after a delay of $1/f$ second. This delay is inevitable because, to sense a dull target against a bright, infrared hot sky background, the seeker must accumulate enough photons from the target over a large number, for example, 100, of frames accumulated in a $1/f$-second sample interval. The inertial LOS angles θ_y and θ_z (both small, less than 1 deg) are then obtained by combining θ_{ys} and θ_{zs}, respectively, with the gyro measurements θ_{yb} and θ_{zb}, stored in a buffer and delayed by $1/f$-second sample period to be in sync with the seeker measurements. Also, a delta-velocity

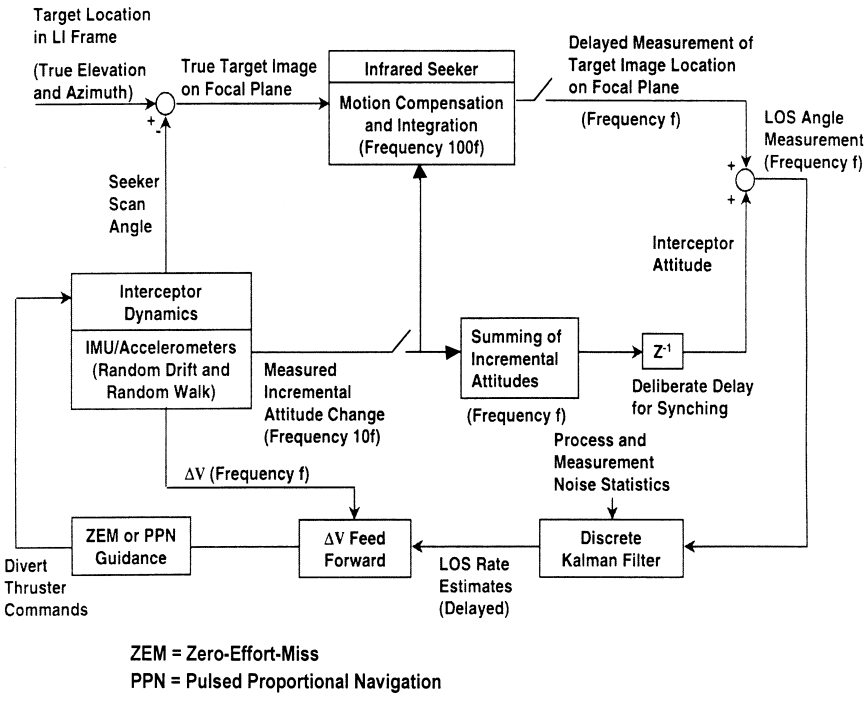

Fig. 2 LOS angle measurement with a scanning seeker and an IMU; interceptor guidance architecture.

feedforward scheme referenced in Fig. 2 compensates, in guidance, for the aforementioned measurement delay of $1/f$ second (Ref. 8).

Seeker Measurement Noise

The seeker measurements θ_{ys} and θ_{zs} are actually corrupted with a zero-mean white noise, denoted $w_{\alpha,\text{skr}}$, of variance σ^2_{skr}: $\theta_{\alpha s,m} = \theta_{\alpha s} + w_{\alpha,\text{skr}}$, where $w_{\alpha,\text{skr}} \sim (0, \sigma^2_{\text{skr}})$ and $\alpha = y, z$. The noise arises from optical diffraction and aberration in optics. The facile white noise assumption is not in depth, however, because the determination of its standard deviation σ_{skr} is a daunting task, nor is the noise exactly white. It depends on the extraordinarily complex electrooptic process described earlier of seeker pixels at $100f$ Hz operating frequency, gyro measurements at $10f$ frequency, motion compensation and integration, optical phenomena of pixel filling and sweeping, etc.[13] All of these processes are beyond the scope of this paper, but the seeker noise, as their fallout, will be illustrated.

Gyro Scan Errors

The seeker scan motion enhances the signal-to-noise ratio of the focal plane measurements. Suppose the scan is rectilinear, a limit-cycle motion effected by a reaction jet controller, and that the scan rate (the limit-cycle rate) is constant, equal to $\pm\omega_s$, reversing its sign periodically at some low frequency consistent with the seeker operation and the target radiance properties. Because of an effective one sample delay of $1/(10f)$ second in the gyro measurements explained earlier, the measured scan rate at the time of scan reversal, according to Eq. (9), differs somewhat from the true scan rate. Therefore, the rate error exhibits pronounced spikes over a 2.5-ms sample period, and the spike amplitudes may be as much as, but generally less than, $\pm 2\omega_s$. These rate error spikes, shown in Ref. 14, cause a difference of no more than a bias of $\pm\omega_s \Delta t_{\text{gyro}}$ between the actual scan angle and the measured scan angle. Here, Δt_{gyro} is the gyro measurement sample period, equal to 2.5 ms in this study. More specifically, this error has the form of a rectangular wave of varying height, and the height depends on at which of the nine most recent 2000-Hz samples of the measured delta-scan angles the seeker reverses its scan direction and on attitude dynamics and control of the interceptor. The scan error, denoted ν_{scan}, will not be mathematically modeled here but it is shown later. From the standpoint of LOS rate estimation, a rectangular bias error in a scan angle estimate is unimportant, but its sign change at each scan reversal causes a deterministic step change in the LOS angle measurement error at the scan frequency, which, in turn, causes a cyclic oscillation in the LOS rate estimates from the Kalman filter.

In this study, the interceptor scans about the elevation y axis. With the instantaneous gyro drift angle ν_{dr} and random walk ν_{rw}, the measured y-attitude angle $\theta_{yb,m}$ about the elevation axis is $\theta_{yb,m} = \theta_{yb} + \nu_{y,\text{dr}} + \nu_{y,\text{rw}} + \nu_{\text{scan}}$. Combining the seeker measurement $\theta_{ys,m} = \theta_{ys} + w_{y,\text{skr}}$ with the gyro measurement, the total measured LOS elevation angle $\theta_{y,m}$ is

$$\theta_{y,m} = \theta_{yb,m} + \theta_{ys,m} = \theta_y + \nu_{\text{scan}} + \nu_{y,\text{dr}} + \nu_{y,\text{rw}} + w_{y,\text{skr}} \quad (10)$$

The azimuth measurement equation does not have the scan angle error and is given by

$$\theta_{z,m} = \theta_{zb,m} + \theta_{zs,m} = \theta_z + \nu_{z,\text{dr}} + \nu_{z,\text{rw}} + w_{y,\text{skr}} \quad (11)$$

Illustrations

Scan Error Noise

Consider a seeker with an ideal scan rate about the elevation axis of $\omega_s = \pm 34$ mrad/s with a limit cycle period of 0.36 s. Assume a reaction jet attitude controller with an instantaneous impulse to change periodically the sign of the scan rate at an interval of 0.18 s. The gyro exhibits a rate error for a 2.5-ms sample period only for every scan reversal. Because the Kalman filter operates at 40 Hz (25 ms), the filter is not exposed to the scan rate error directly, but it encounters a bias angle error ν_{scan} in the measurement of the scan angle (Fig. 3). This bias error alternates its sign; its magnitude varies from scan to scan as explained earlier. The net change in the bias scan angle error at the time of turnaround varies from 50 to 80 μrad, as seen in Fig. 3. For a 40-Hz filter, a sudden change in the bias error creates an effective input of 2–3.2 mrad/s (equal to 50–80 μrad/0.025 s) LOS rate measurement error.

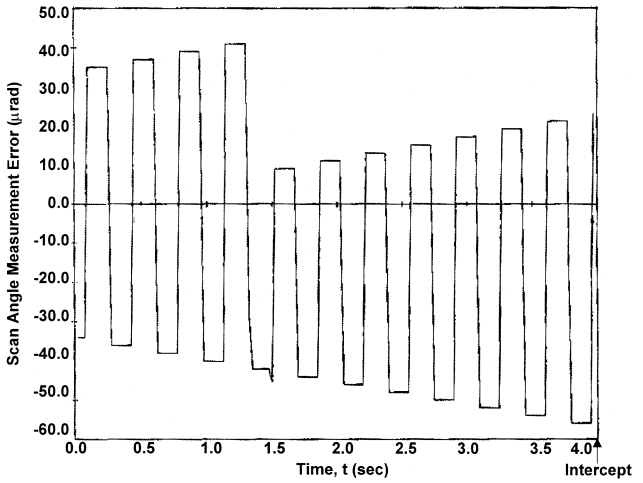

Fig. 3 Difference between measured and the true scan angles (40 Hz).

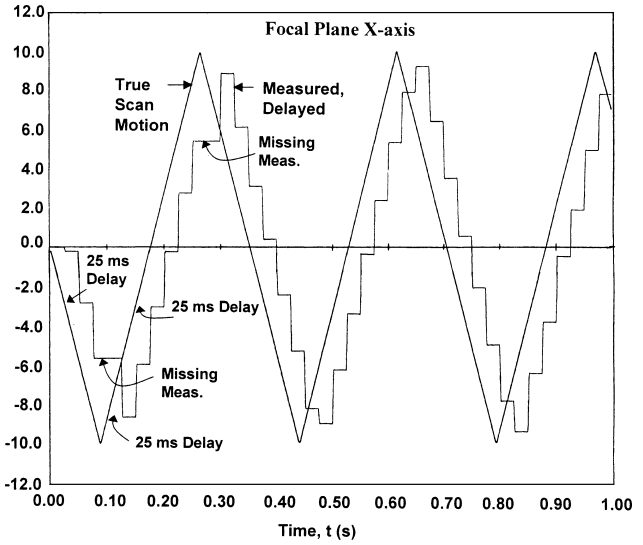

Fig. 4 True and one-sample delayed measured location of the target on the focal plane: x coordinate.

Seeker Noise

The target image location on the seeker focal plane depends on both the instantaneous scan angle of the focal plane and the inertial location of the target. For simplicity, suppose the interceptor is on a collision course; that is, the miss distance is zero. Then, the x component of the true target image streak on a scanning focal plane and its one-sample-delayed discrete measurement, both vs time, are shown in Fig. 4 in arbitrary units. These results are obtained from a sophisticated code, developed over years, that simulates electro-optic processes of the seeker and motion compensation and integration of the target image using incremental attitude measurements from a strapdown gyro, as explained earlier. The results in Fig. 4 are for a gyro with zero drift and zero random walk. (The results with gyro errors are shown in the next subsection.) The difference between the true location of the target image at the start of a 40-Hz frame and its measured location determined at the end of the same 40-Hz frame for both axes of the focal plane is shown in Fig. 5. These errors are generally within ± 0.1 units, although once in a way they are far outside when, during a turnaround, the target image does not cross enough (two) pixels and the seeker software is then unable to locate the target image on the focal plane. The focal plane measurement errors in Fig. 5, transformed into the interceptor lateral axes, are what were modeled earlier as white noise in the seeker measurements.

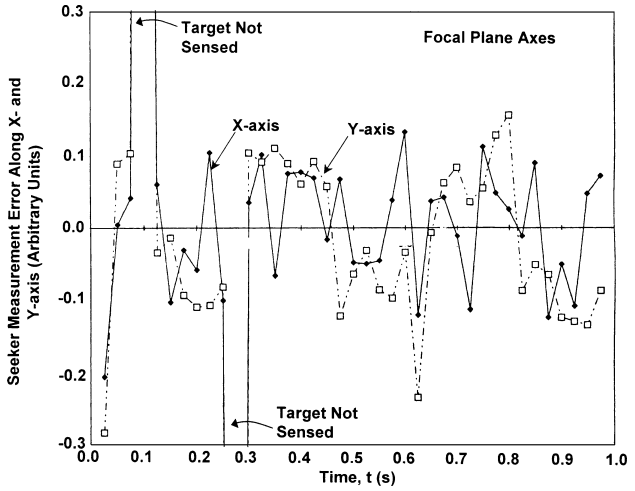

Fig. 5 Seeker measurement error in centroiding the target image on the *xy* focal plane.

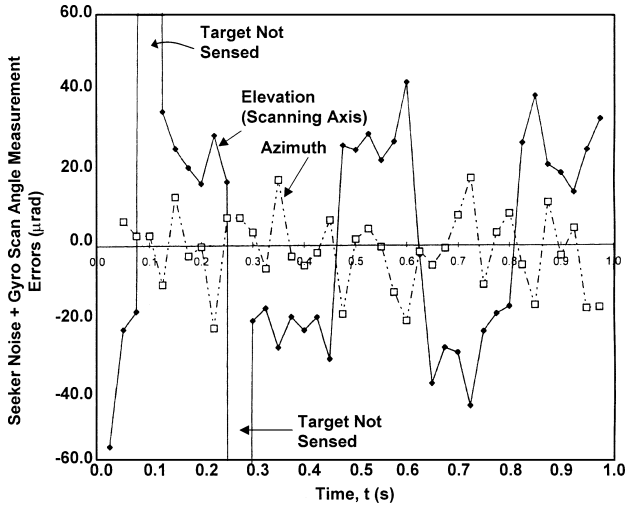

Fig. 6 Seeker noise plus scan angle measurement error about elevation axis and seeker noise about azimuth axis (gyro drift and random walk zero).

Composite Seeker and Gyro Errors

The focal plane error transformed into the interceptor lateral axes and combined with the bias scan angle error of gyros without drift and random walk are shown in Fig. 6 for both azimuth and elevation angles. Because of the additional scan error about the elevation axis, the resultant elevation measurement error is biased and much larger than the azimuth measurement error. Figure 7 shows the composite elevation error until the closest approach at $t = 4$ s ($t_{go} = 0$) and compares it with the gyro scan error illustrated earlier in Fig. 3. In Fig. 7, the scan motion is terminated at $t = 3.5$ s because, by then, the target image has bloomed and it covers several pixels on the focal plane. We observe in Fig. 7 that the combined elevation measurement error is approximately equal to the gyro scan error. In contrast, the azimuth measurement error in Fig. 6 is essentially a white noise, generally less than 20 μrad, with $\sigma_{skr} \approx 8$ μrad. An estimate of the seeker rate error in azimuth, then, is $\sqrt{2} \times 8$ μrad/0.025 s ≈ 0.5 mrad/s.

In these examples, the error parameters of the Litton LN-200 inertial measurement unit (IMU) are used. The IMU gyro's drift rate is 5 μrad/s and standard deviation σ_{rwr} of the gyro random walk rate is 29 μrad/$\sqrt{s}$. For a guidance sample period of 25 ms, the random walk adds incrementally a measurement error of $\sqrt{(\sigma_{rwr}^2 \times 0.025 \text{ s})} = 4.6$ μrad (1σ). The meandering gyro random walk with superimposed seeker azimuth error (seen in Fig. 6) is shown in Fig. 8 for the same 4-s endgame scenario. From the standpoint of motion compensation and integration (MCI) process

Table 2 Effective LOS rate error input to the Kalman filter (40 Hz)

Parameter	Scan rate error of IMU, mrad/s	Seeker rate error, mrad/s	Random walk rate of IMU, mrad/s	Drift rate of IMU, mrad/s
Elevation	2–3.2	0.5	0.2	0.005
Azimuth	0	0.5	0.2	0.005

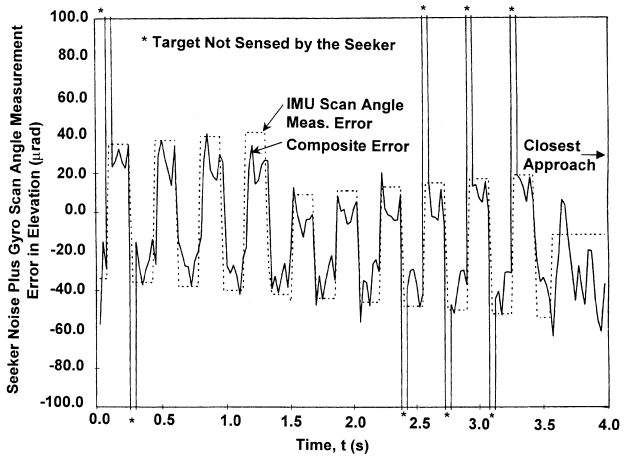

Fig. 7 Composite elevation measurement error compared with scan angle measurement error of the gyro.

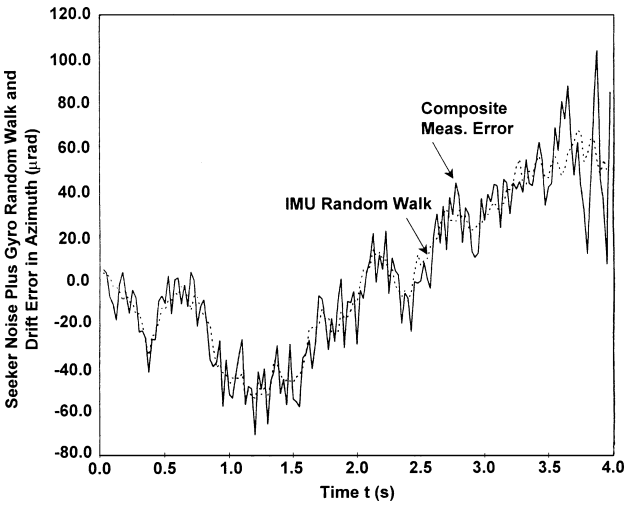

Fig. 8 Composite measurement error of the seeker and the gyro in azimuth, compared with the gyro random walk and drift.

for identifying the target image, only the incremental random walk, 4.6 μrad (1σ), in any 25-ms period adds on to the seeker measurement noise; however, this error is negligible compared to the seeker's own "white" electrooptic noise shown in Fig. 6 for azimuth. The random walk about the elevation axis similarly affects the elevation error, shown in Fig. 7.

LOS Rate Error Input to a Kalman Filter

All earlier elucidated sources of LOS rate errors are collected in Table 2: The LOS rate errors caused by the white electrooptic noise, the seeker scan rate measurement error of the gyro about the elevation axis, and the gyros' drift rate and random walk rate. These input rate errors enter the Kalman filter indirectly via inertial LOS angle measurement by the seeker and the gyro. The LOS rate error arising from random walk in a guidance sample period is $\sqrt{[\sigma_{rwr}^2/(0.025 \text{ s})]} = 0.18$ mrad/s. However, as far as miss distance is concerned, it is the LOS rate estimation error, not LOS rate input error, that is of paramount importance. This is discussed next.

Table 3 Miss distance for $t_{go,ineff} = 0.05$ and 0.1 s

Axis	LOS rate estimation error, μrad/s	Time-to-go error δt_{go}, s	ZEM_{nom}, cm		$ZEM_{nom} + \delta ZEM$, cm	
			$T_L = 0.05$ s	$2T_L = 0.1$ s	$T_L = 0.05$ s	$2T_L = 0.1$ s
Elevation	200	0.005	1.5	5	2	7
Azimuth	100		1.5	5	2	5
RSS			2.1	7	2.8	8.6
Elevation	200	0.2	1.5	5	6	14
Azimuth	100		1.5	5	6	13.5
RSS			2.1	7	8.5	19.5

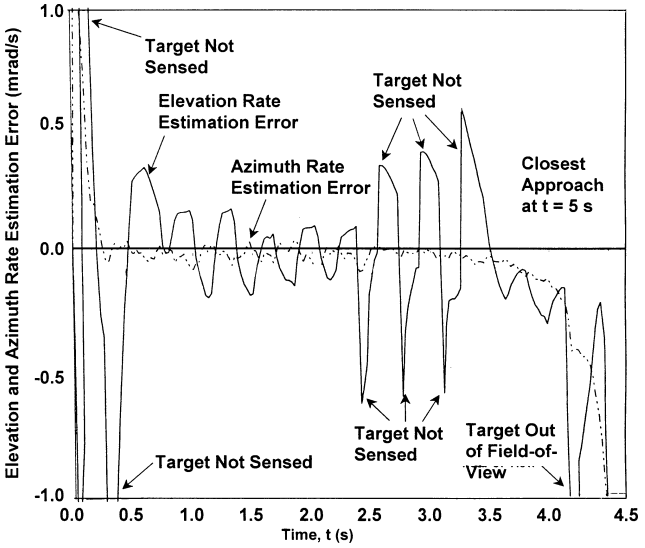

Fig. 9 Azimuth and elevation rate estimationn error of Kalman filter (guidance inactive).

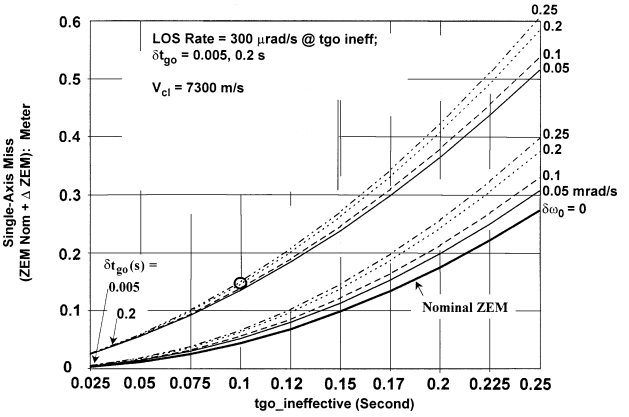

Fig. 10 Nominal plus 1σ miss distance estimation uncertainty vs $t_{go,ineffective}$.

LOS Rate Estimation Errors

This error depends on the filtration of the input errors just discussed by a Kalman filter. This filtration is predicated on the LOS angle dynamics, Eq. (3), and the process noise matrix that statistically embodies modeling errors. A frequency- or time-domain analysis of the estimation process in not our intention; we illustrate the azimuth and elevation LOS rate estimation errors via simulation results in Fig. 9. Unlike the scenario of Figs. 7 and 8, the miss distance for the scenario in Fig. 9 is nonzero but the guidance is turned off. Hence, the true LOS rates, their estimates, and the estimation errors diverge as t_{go} decreases. Compared with the input scan rate error (Table 2) of 2–3.2 mrad/s in elevation, the elevation rate estimation error in steady state is ~0.2 mrad/s. This error is larger during the Kalman filter transients near $t = 0$ and when the target image did not form during a scan reversal. Near the closest approach at $t = 5$ s, because the guidance is inactive, the target exits the field of view. The steady-state azimuth rate estimation error is below 0.1 mrad/s.

V. Comparison of Analytical Miss Distance Predictions with Monte Carlo Results

Figure 10 shows ZEM_{nom} (nominal) and $ZEM_{nom} + \delta ZEM$ when the LOS rate at a given $t_{go,ineff}$ (0.025–0.25 s) is 300 μrad/s, equal to the LOS rate threshold, and δt_{go} error is 0.005 or 0.2 s. Figure 10 shows the miss distances for the LOS rate estimation errors $\delta\omega_0 = 0.05, 0.1, 0.2$, and 0.25 mrad/s. Here δZEM is predicted by using Eq. (6) and ZEM_{nom} at $t_{go,ineff}$ is calculated from $ZEM = \omega t_{go}^2 V_{cl}$. In statistical analyses, the miss distance uncertainty δZEM would be equivalent to a 1σ standard deviation of the nominal ZEM.

Because seeker processes impose one guidance sample lag and because the flight computer delays transporting the LOS rate estimate to the guidance module by an additional sample period, the total lag is two guidance sample periods ($T_L = 0.05$ s). According to Table 1 then, $t_{go,ineff} = T_L$-$4T_L = 0.05$–0.20 s. Consequently, Fig. 10 considers $t_{go,ineff}$ from 0.025 to 0.25 s. The δt_{go} error is a function of the assets (ground-tracking radars, satellites, etc.) employed to determine the in-flight target updates. Specifically, if the GPS satellites are employed, $\delta t_{go} = 0.005$ s, and if a ground tracking radar is used, then $\delta t_{go} = 0.2$ s. The guidance system suppresses the estimated LOS rate in the neighborhood of its threshold, and as seen in Fig. 9, the LOS rate estimation error will be about 0.1–0.2 mrad/s. Accordingly, in Fig. 10, it is assumed that when $t_{go} = t_{go,ineff}$, the true LOS rate is equal to the threshold, 300 μrad/s, and the LOS rate estimation errors range from 0.05 to 0.25 mrad/s. The closing velocity V_{cl} is 7300 m/s and $\delta V_{cl} = 7.3$ m/s, and therefore, its contribution to δZEM is negligible. For all of these parameters, Fig. 10 shows both ZEM_{nom} and $ZEM_{nom} + \delta ZEM$ vs $t_{go,ineff}$. The two miss distances vary quadratically with $t_{go,ineff}$. For example, for $t_{go,ineff} = 2T_L = 0.1$ s (according to the Nyquist criterion, Table 1), when the ground-tracking assets are used with $\delta t_{go} = 0.2$ s, the miss distance corresponding to the elevation axis for $\delta\omega = 0.2$ mrad/s is 14 cm. Likewise, the miss distance corresponding to the azimuth axis for $\delta\omega = 0.1$ mrad/s is 13.5 cm. The rss miss is then 19.5 cm. These results, as well as those for $\delta t_{go} = 0.005$, are summarized in Table 3. It is evident from these results that the predicted miss distances will be optimistic if δt_{go} error is ignored (~8 cm for $\delta t_{go} = 0$ compared to ~20 cm for $\delta t_{go} = 0.25$ s).

This study stemmed from the need to be able to predict by back-of-the-envelope calculations reliable miss distances accounting for all realistic error soruces. This need arises because building a huge, comprehessive six-degree-of-freedom (6-DOF) simulation is a multiyear task and generating miss distances based on Monte Carlo runs entails extraordinary efforts. Therefore, it is instructive to compare the miss distances predicted by the two approaches. Figure 11 shows the rss miss distance vs a scalar factor q of the process noise matrix of the Kalman filter. These results are based on a 6-DOF end-to-end simulation. Two cases[8] are considered in Fig. 11: 1) a constant process noise matrix multiplied with a factor q and a constant transition matrix and 2) both matrices varying with time as a function of t_{go}. For both cases, the minimum miss distance is ~17–18 cm against the prediction of 19.5 cm from the simple analysis, a

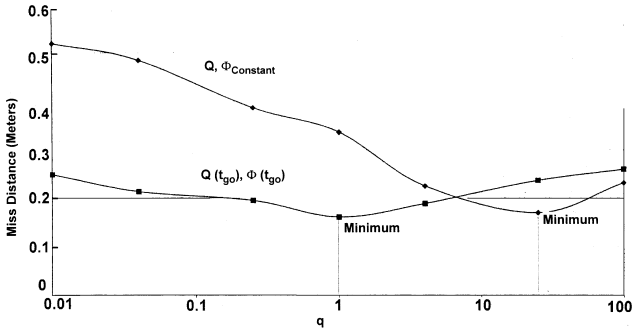

Fig. 11 Miss distance vs the process noise matrix coefficent q for time-invariant and time-varying process noise matrix Q and transition matrix Φ.

remarkable agreement in the two approaches indeed, despite that the two approaches involve vastly different orders of labor.

VI. Conclusions

With use of the proceeding analysis, the expected miss distance and its uncertainty can be calculated for the known bounds of seeker latencies, time-to-go error, LOS rate estimation error, and the LOS rate at a time-to-go where due to noise and delays the guidance becomes ineffective. These predictions compare remarkably well with the miss distances obtained from a comprehensive 6-DOF simulation and hardware-in-the-loop laboratory tests. The analysis presented here is valuable because it facilitates a reliable back-of-the-envelope determination of miss distance for given hardware and software guidance parameters, which obviates the need in the early stages of a program for developing a sophisticated, comprehensive trajectory simulation of guidance, navigation, and control system and Monte Carlo runs. More specifically, the relationships developed here can be used to determine the hardware parameters such as divert thrust and minimum impulse bit and software parameters such as LOS rate threshold, LOS rate estimation accuracy requirement, range and range rate accuracy requirement (that is, acceptable time-to-go error), and seeker latencies to meet a miss distance requirement. Also, the analysis decreases significantly the efforts of the designer or analyst and provides prompt insight and tools to evaluate soundness of the Monte Carlo and laboratory test results.

References

[1]Alpert, J., "Miss Distance Analysis for Command Guided Missiles," *Journal of Guidance, Control, and Dynamics*, Vol. 11, No. 6, 1988, pp. 481–487.

[2]Nesline, F. W., and Zarchan, P., "Miss Distance Dynamics in Homing Missiles," *AIAA Guidance and Control Conference*, AIAA, New York, 1984, pp. 84–98.

[3]Salmon, D. M., and Heine, W., "Reachable Sets Analysis—An Efficient Technique for Performing Missile/Sensor Tradeoff Studies," *AIAA Journal*, Vol. 11, No. 7, 1973, pp. 927–931.

[4]Zarchan, P., "When Bad Things Happen to Good Missiles," *AIAA Guidance, Navigation, and Control Conference*, AIAA, Washington, DC, Pt. 2, 1993, pp. 765–773.

[5]Spencer, A., and Moore, W., "Design Trade-Offs for Homing Missiles," AIAA Paper 92-2755, May 1992.

[6]Lawrence, R. V., "Interceptor Line-of-Sight Rate Steering: Necessary Conditions for a Direct Hit," *Journal of Guidance, Control, and Dynamics*, Vol. 21, No. 3, 1998, pp. 471–476.

[7]Murtaugh, S. A., and Criel, H. E., "Fundamentals of Proportional Navigation," *IEEE Spectrum*, Vol. 3, Dec. 1966, pp. 75–85.

[8]Hablani, H. B., "Pulsed Guidance of Exoatmospheric Interceptors with Image Processing Delays in Angle Measurements," AIAA Paper 2000-4272, Aug. 2000.

[9]Nesline, F. W., and Zarchan, P., "Line-of-Sight Reconstruction for Faster Homing Guidance," *Journal of Guidance, Control, and Dynamics*, Vol. 8, No. 1, 1985, pp. 3–8.

[10]Balakrishnan, S. N., and Speyer, J. L., "Coordinate-Transformation-Based Filter for Improved Target Tracking," *Journal of Guidance, Control, and Dynamics*, Vol. 9, No. 6, 1986, pp. 704–709.

[11]Gurfil, P., Jodorkovsky, M., and Guelman, M., "Finite-Time Stability Approach to Proportional Navigation System Analysis," *Journal of Guidance, Control, and Dynamics*, Vol. 21, No. 6, 1998, pp. 853–861.

[12]Shneydor, N. A., *Missile Guidance and Pursuit: Kinematics, Dynamics and Control*, Horwood, Chichester, England, U.K., 1998, Secs. 6.5.4, 8.6.4.

[13]Vandersteen, A., and Kelley, B. "Longwave Infrared (LWIR) Advanced Technology Seeker (LATS) Status," AIAA Paper 92-0988, Feb. 1992.

[14]Hablani, H. B., and Pearson, D. W., "Determination of Guidance Parameters of Exoatmospheric Interceptors via Miss Distance Error Analysis Avoiding Monte Carlos," *AIAA Guidance, Navigation, and Control Conference*, AIAA, Reston, VA, 2001, pp. 1393–1409.